

8 Search for the rare decay $\mu^+ \rightarrow e^+ e^- e^+$

R. Gredig, P. Robmann, and U. Straumann

in collaboration with University of Geneva, Paul Scherrer Institute, ETH Zürich, University of Heidelberg
(Mu3e Collaboration)

Neutrino oscillations, as observed by experiments such as SuperKamiokande [1], SNO [2], and KamLAND [3] are a direct proof of lepton flavour violation (LFV). Charged LFV (CLFV) would lead to $\mu \rightarrow e$ and $\tau \rightarrow \mu$ transitions without neutrinos in the final state. In the standard model CLFV can be induced by neutrino mixing but such processes are highly suppressed by the tiny neutrino masses. The observation of CLFV would therefore directly signal physics beyond the standard model. Muon number violation has already been searched in different channels (see Tab. 8.1). When these processes would be observed their relative strengths would guide the attempts to identify the underlying mechanism.

TAB. 8.1 – Experimental upper limits on the branching ratios B of LFV muon decays

Decay channel	Experiment	B upper limit	Ref.
$\mu \rightarrow e\gamma$	MEGA	1.2×10^{-11}	[4]
	MEG	2.4×10^{-12}	[5]
$\mu \rightarrow eee$	SINDRUM	1.0×10^{-12}	[6]
$\mu^- \text{Au} \rightarrow e^- \text{Au}$	SINDRUM II	7×10^{-13}	[7]

A new $\mu^+ \rightarrow e^+ e^- e^+$ search at PSI ultimately aims at a sensitivity down to $B < 10^{-16}$ [8], four orders of magnitude beyond the 26 year old SINDRUM result. The setup (see Fig. 8.1) contains cylindrical layers of silicon pixels and scintillating fibres, placed in a solenoidal magnetic field.

In a first phase, ready to take data by 2016, the setup will include the central pixel detectors, the fibre tracker, and one complete set of recurl stations and the beam-intensity will be $10^8 \mu^+ / \text{s}$. Assuming the phase I detector

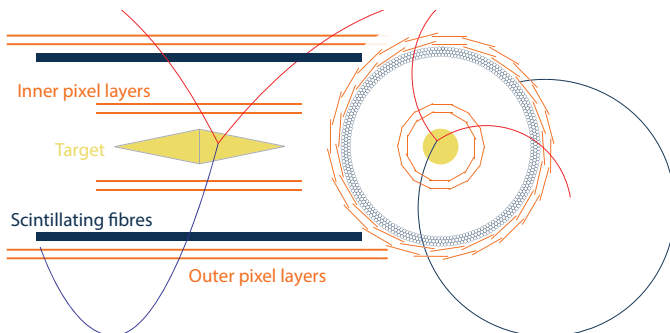


FIG. 8.1 – Central region of the Mu3e setup in the zy and xy projections. The central fibre tracker consists of three layers of $250 \mu\text{m}$ fibres with a length of 36 cm.

works as expected, phase II components should be ready in 2017. There will be two sets of recurl stations and a new muon beam line should give at least one order of magnitude larger stop rate.

- [1] Y. Fukuda *et al.* (Super-Kamiokande Collaboration), Phys. Rev. Lett. 81 (1998) 1562.
- [2] Q.R. Ahmad *et al.* (SNO Collaboration), Phys. Rev. Lett. 87 (2001) 071301.
- [3] K. Eguchi *et al.* (KamLAND Collaboration), Phys. Rev. Lett. 90 (2003) 021802.
- [4] M. L. Brooks *et al.* (MEGA Collaboration), Phys. Rev. Lett. 83 (1999) 1521.
- [5] J. Adam *et al.* (MEG Collaboration), Phys. Rev. Lett. 107 (2011) 171801.
- [6] U. Bellgardt *et al.* (SINDRUM Collaboration), Nucl. Phys. B299 (1988) 1.
- [7] W. Bertl *et al.* (SINDRUM II Collaboration), Eur. Phys. J. C47 (2006) 337.
- [8] A. Blondel *et al.* (Mu3e Collaboration), *Research Proposal for an Experiment to Search for the Decay $\mu \rightarrow 3e$* , submitted to PSI (2013), ArXiv 1301.6113.

8.1 Scintillating Fibres

The University of Zürich, in close collaboration with the University of Geneva and the ETH Zürich, is strongly involved in the R&D for the scintillating fibre tracker which is part of the proposed detector. The fibres are read out with silicon photomultipliers (SiPM) which allow a suf-

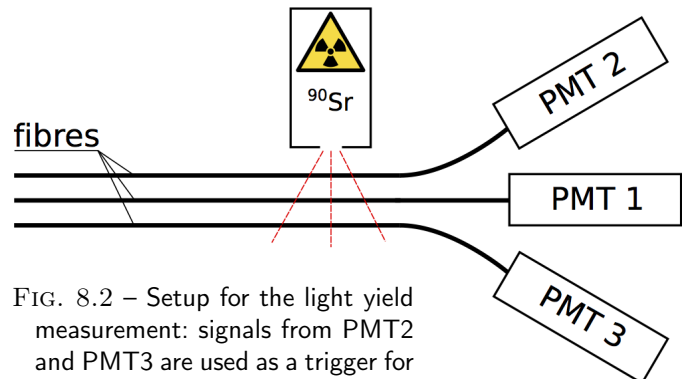


FIG. 8.2 – Setup for the light yield measurement: signals from PMT2 and PMT3 are used as a trigger for the measurement of the number of photo-electrons in PMT1.

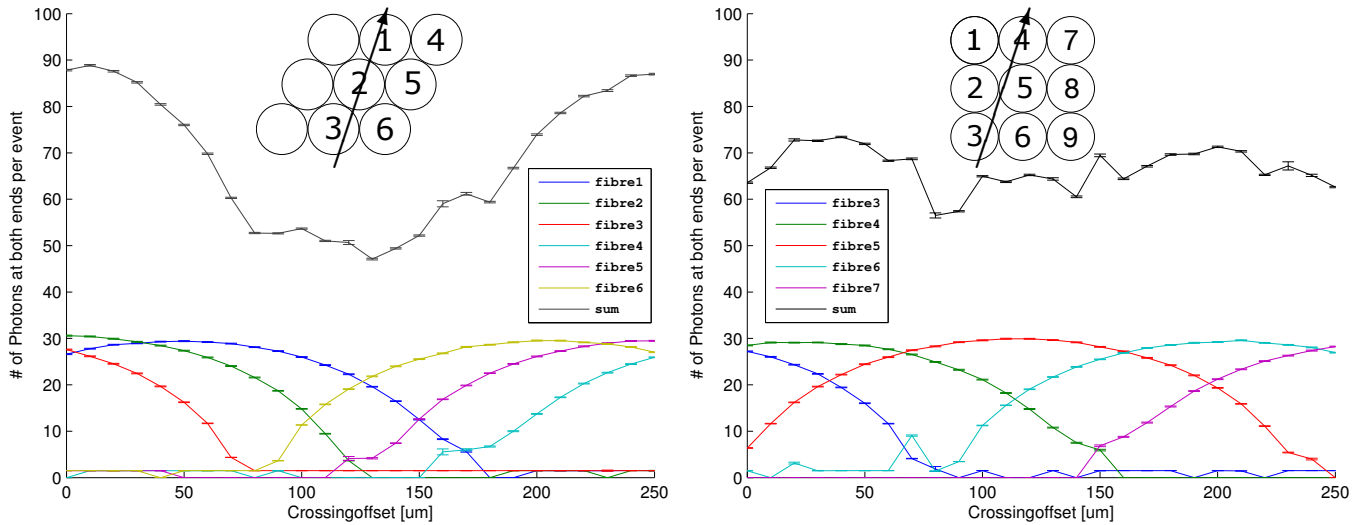


FIG. 8.3 – Predicted number of photons versus positron crossing position at the most likely crossing angle for two alternative staggering geometries as indicated by the insets; the trajectory corresponding to zero crossing position is shown too.

ficiently dense staggering and can be operated in high magnetic fields.

Detailed simulation studies of the light propagation within the fibres have been completed resulting in a parametrization of the photon yield and time distribution over the detector surface to be used as input in the full event simulation. The simulation has been verified with a test setup consisting of three 250 μm fibres irradiated with a ^{90}Sr source (see Fig. 8.2). A coincidence between the two outer fibres is used as trigger and the signal of the middle fibre is registered. The simulation includes the passive support material and accounts for the energy spectrum of the source. The observed light yield is $\approx 20\%$ below the prediction which we consider satisfactory, given the large number of reflections. The predicted time resolution of about 400 ps has been confirmed by a test measurement at the University of Geneva.

Next, a study was made of the fibre configuration since the photon yield depends on the way how the ribbons are staggered (Fig 8.3). The final configuration will be a trade-off between light yield, multiple scattering and mechanical feasibility.

8.2 Readout Electronics

Together with the University of Geneva, multi channel readout electronics has been developed. For maximum flexibility the SiPM sensors have been separated from the amplifier board itself allowing to test different sensors and amplifier boards. Fig 8.4 shows a daughterboard with a 4x4 SiPM sensor-array. This board can be connected to an amplifier array with 16 channels (Fig. 8.5). Two of these sets can be combined to read out 32 fibres from a fibre ribbon. The amplifier electronics is designed in such a way that it can later be integrated in an ASIC design. As the final detector will have thousands of channels, the electronics need to be highly integrated because of spatial limitations.

First experiences at a DESY electron test beam helped to improve the data acquisition software and the readout electronics. From the next beam tests at PSI first results of the fibre ribbon performance in beam are expected.

22

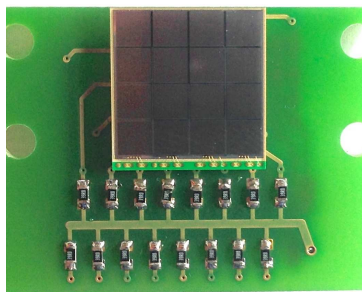


FIG. 8.4 – Daughterboard with a 4x4 Hamamatsu array.

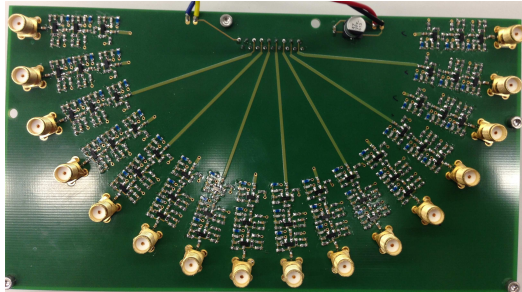


FIG. 8.5 – 16-channel motherboard.

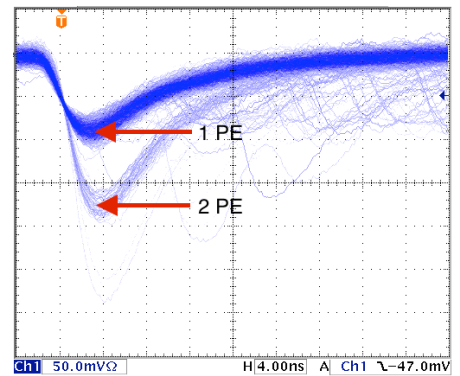


FIG. 8.6 – SiPM signals showing clean one and two photoelectron events.